

Multitasking with Chemical Fuel: Dissipative Formation of a Pseudorotaxane Rotor from Five Distinct Components

Amit Ghosh, Indrajit Paul, and Michael Schmittel*

Cite This: *J. Am. Chem. Soc.* 2021, 143, 5319–5323

Read Online

ACCESS |

Metrics & More

Article Recommendations

Supporting Information

ABSTRACT: A 3-fold complete self-sorted library of dynamic motifs was integrated into the design of the pseudorotaxane-based rotor $[\text{Zn}(2\cdot\text{H}^+)(3)(4)]^{2+}$ operating at $k_{298} = 15.4$ kHz. The rotational motion in the five-component device is based on association/dissociation of the pyridyl head of the pseudorotaxane rotator arm between two zinc(II) porphyrin stations. Addition of TFA or 2-cyano-2-phenylpropanoic acid as a chemical fuel to a zinc release system and the loose rotor components 2–4 enabled the liberated zinc(II) ions and protons to act in unison, setting up the rotor through the formation of a heteroleptic zinc complex and a pseudorotaxane linkage. With chemical fuel, the dissipative system was reproducibly pulsed three times without a problem. Due to the double role of the fuel acid, two kinetically distinct processes played a role in both the out-of-equilibrium assembly and disassembly of the rotor, highlighting the complex issues in multitasking of chemical fuels.

Chemical fuels play a central role in setting up dissipative systems on the molecular level, e.g., in host–guest systems,^{1–3} transient switching,^{4–6} ratcheted directional motion,^{7,8} catalysis using molecular machines,⁹ and the generation of supramolecular materials^{10–14} and self-replicators.¹⁵ However, to achieve feedback control as in living organisms, it would be desirable to have man-made functional multicomponent devices be dissipatively generated to perform vital tasks and to disappear after completion of their work.^{16–19} Here, we demonstrate the out-of-equilibrium self-assembly and operation of a five-component rotor by a single chemical fuel. In contrast to fueled homo-oligomeric aggregation,¹⁰ multitasking of the fuel is required, as distinct binding events need to be set up for the assembly of five components.

While the potential of synthetic molecular machines has been widely recognized,^{20–24} most of them are covalently assembled, whereas biological machines are typically composed of different components.^{25,26} Except for a limited amount of cases,^{27–34} artificial multicomponent machinery remains rare, due to a lack of tools for controlling their dynamics parallel in space and time.³⁵ Capitalizing on a small number of dynamic orthogonal metal–ligand interactions, our group has started to prepare diverse multicomponent stand-alone devices³⁶ and functional multicomponent networks.^{37,38} Thus, fueling metal ion release would open a multitude of opportunities due to the broad availability of metal-ion dependent devices.²⁰

To date, the only artificial multicomponent system commanded by chemical metal-ion pulses is a lithium(I)-based AND gate³⁹ designed as a communicating network. For the present project we envisaged that acid **6**, developed by Di Stefano et al.,⁴⁰ as chemical fuel should initiate two out of three binding events in the dissipative formation of the five-component pseudorotaxane-based rotor $5 = [\text{Zn}(2\cdot\text{H}^+)(3)(4)]^{2+}$ from its constituents by (i) protonating ligand **2** (for pseudorotaxane formation) and (ii) liberating zinc(II) ions from $[\text{Zn}(\mathbf{1})]^{2+}$ (Figure 1).

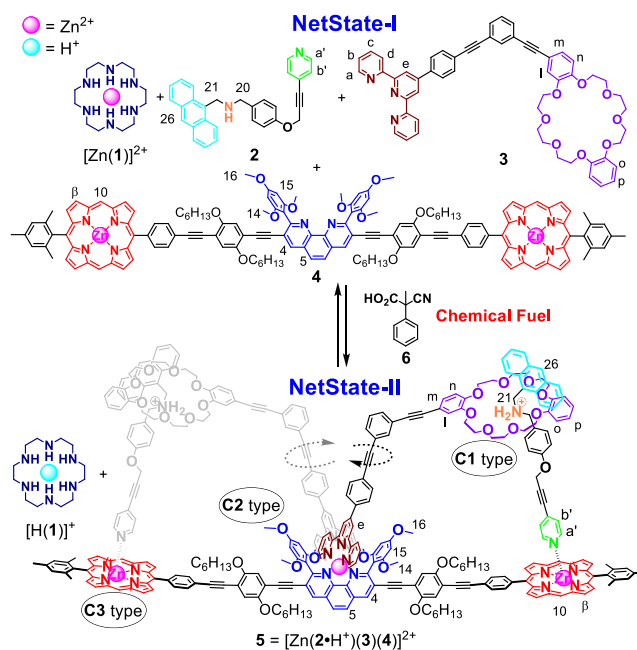


Figure 1. Chemical communication generates a transient rotor.

Self-sorting^{41,42} as a key technology to assemble multicomponent devices^{27–34} is based on the use of multiple orthogonal dynamic interactions. Lately, we have shown that the HETTAP⁴³ (Heteroleptic Terpyridine and Phenanthroline)

Received: February 19, 2021

Published: March 31, 2021



linkage is fully orthogonal to the pyridine→zinc(II) porphyrin ($N_{py} \rightarrow ZnPor$) binding but never in combination with a pseudorotaxane-type complexation motif.⁴⁴ Whereas the pseudorotaxane unit has been the basis of many intricate assemblies⁴⁵ and interlocked molecular machines,^{46–48} its utility in multicomponent molecular devices is still unexplored. Here, the pseudorotaxane motif serves not only as a dynamic corner of the five-component rotor along with the HETTAP and $N_{py} \rightarrow ZnPor$ complexation but also as an anchor point for its out-of-equilibrium formation.

Prior to designing detailed components of the rotor, three fully orthogonal binding motifs were required with at least one being responsive to an acid fuel. In this regard, we identified complexes **C1**, **C2**, and **C3** as promising candidates (Figure 2)

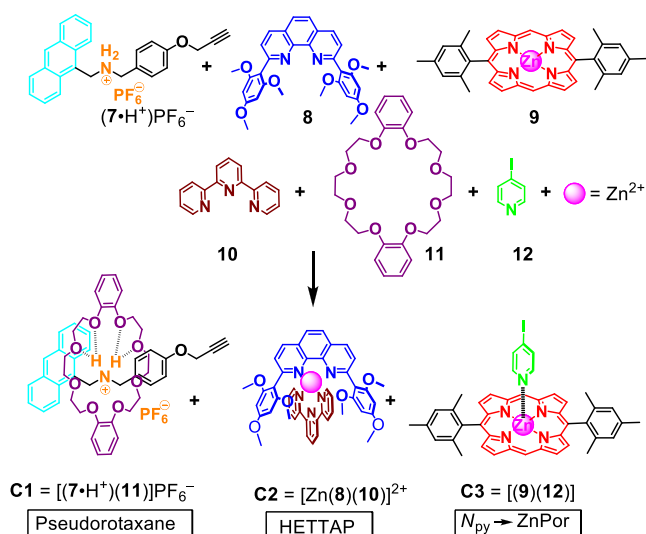


Figure 2. Complexation motifs used in the five-component pseudorotaxane rotor.

due to their interference-free self-sorting. As shown in Figure 2, mixing of stoichiometric amounts of (7·H⁺)PF₆[−], 8–12, and Zn(OTf)₂ (1:1:1:1:1:1:1) generated the pseudorotaxane **C1** = [(7·H⁺)(11)]PF₆[−] (log *K* = 4.74 ± 0.20, Supporting Information, Figure S68) and the strong HETTAP complex **C2** = [Zn(8)(10)]²⁺ (log β ≈ 15.0, Supporting Information, Figure S70) together with the well-established $N_{py} \rightarrow ZnPor$ complexation motif **C3** = [(9)(12)] (log *K* = 4.31 ± 0.12).⁴⁹

On the basis of this insight, we designed the five components of the rotor: protons, ligands 2, 3, and 4, and zinc(II) ions (Figure 1). First, ligand 4 that contains two zinc(II) porphyrin stations at both terminals and a phenanthroline station in the middle was synthesized according to a known procedure.⁵⁰ The dibenzo-24-crown-8 and terpyridyl motifs were combined in ligand 3, which acts as an axis of rotor 5. The rotator arm 2 was conceived as a secondary amine with an anthracene stopper carrying additionally a pyridine terminal. For the full synthesis of 2 and 3, see Schemes S1 and S2 in the Supporting Information.

When ligands 2, 3, and TFA were mixed (1:1:1) in DCM, the ammonium moiety of the linear component 2·H⁺ (referred to as thread) slid into the macrocycle of ligand 3. As expected, the ¹H NMR spectrum showed the typical upfield shifts of the crown's aromatic proton signals m-H, l-H, and n-H, while the peak at 6.89 ppm corresponding to o-H and p-H split in two sets (Supporting Information, Figure S51). The signals of anthracenyl and benzyl protons 21-H and 20-H, adjacent to

the ammonium moiety, shifted downfield from 4.95 and 4.00 to 5.51 and 5.27 ppm, respectively. The threading was also confirmed by the emergence of multiple sets of cyclic ether protons in the aliphatic region. UV–vis, fluorescence, and ESI-MS (Supporting Information, Figures S67, S72, and S63) further proved the formation of pseudorotaxane [(2·H⁺)(3)] (log *K* = 5.58 ± 0.03, Supporting Information, Figure S69).

The bent geometry of [(2·H⁺)(3)] with its terpyridyl and pyridyl terminals allowed two connections to ligand 4 after addition of Zn(OTf)₂, one via a HETTAP linkage and the other via $N_{py} \rightarrow ZnPor$ binding. The zinc(II) ion set up a strong HETTAP⁴³ complex between the central phenanthroline of 4 and the terpyridyl unit of the pseudorotaxane, whereas the pyridine terminal of rotator [(2·H⁺)(3)] formed an $N_{py} \rightarrow ZnPor$ coordination. The pyridine was expected to move quickly between the two identical ZnPor binding sites, giving rise to rotor 5 (Figure 3a). As expected from the clean self-sorting of

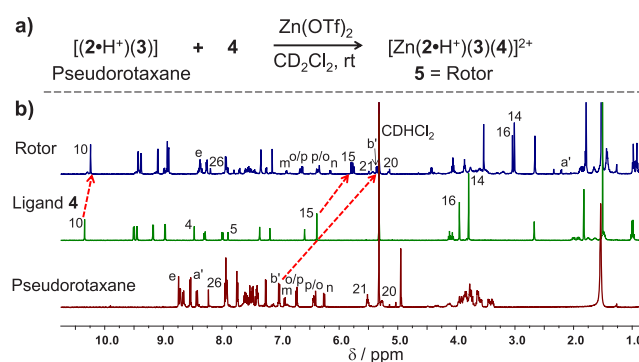


Figure 3. (a) Synthesis of rotor 5. (b) Comparison of partial ¹H NMR spectra (CD₂Cl₂, 400 MHz) of pseudorotaxane [(2·H⁺)(3)], 4, and rotor 5.

the basic building blocks, rotor 5 was furnished quantitatively, as evident from ¹H NMR, ¹H–¹H COSY, DOSY, and electrospray mass spectroscopy (ESI-MS). For instance, ESI-MS peaks at *m/z* = 1908.4 (doubly charged) and 1222.7 (triply charged) attested the formation of [Zn(2·H⁺)(3)(4)]²⁺ (Supporting Information, Figure S65). ¹H NMR analysis showed the characteristic upfield shifts of proton signals 10-H from 10.34 to 10.21 ppm and 15-H from 6.38 to 5.78 ppm, proving the existence of both $N_{py} \rightarrow ZnPor$ and HETTAP complexation (Figure 3b). Similarly, the pyridyl protons a'/b'-H were characteristically shifted upfield from 8.54/7.25 ppm to 2.21/5.36 ppm due to coordination at the ZnPor. The pseudorotaxane linkage was indicated by the signals of protons 21-H and 20-H, adjacent to the ammonium moiety, that appeared at 5.43 and 5.15 ppm. Finally, a single set of ¹H-DOSY signals (*D* = 4.5 × 10^{−10} m² s^{−1}, *r* = 11.8 Å, in CD₂Cl₂) supported the formation of the assembly (Supporting Information, Figure S47).

To measure the exchange frequency in rotor 5, we analyzed the signal (Figure 4a) of proton 10-H, which showed up as a sharp singlet (10.21 ppm) at 25 °C in the variable temperature ¹H NMR. The single set of protons for both porphyrin units attested fast rotation on the ¹H NMR time scale. Diagnostically, at −50 °C, it separated into two singlets (1:1) at 10.30 and 10.19 ppm. The signal at 10.19 ppm was assigned to the pyridine-coordinated ZnPor station, whereas the upfield signal at 10.30 ppm referred to the freely rotating ZnPor. The kinetic analysis provided the exchange frequency *k* at different temperatures, with *k*₂₉₈ = 15.4 kHz. From the Eyring equation, the activation

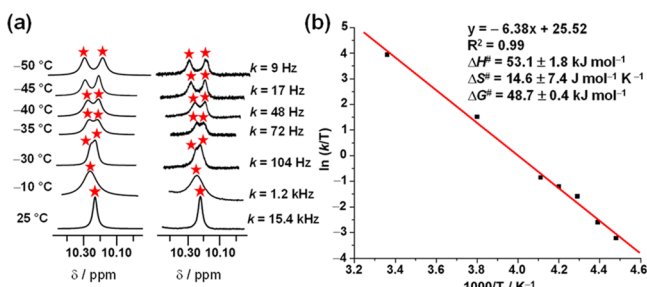


Figure 4. (a) Experimental (right) and simulated (left) variable temperature ^1H NMR spectra of rotor 5 (signal of proton 10-H) and the exchange frequency k . (b) Eyring plot.

parameters were calculated as $\Delta H^\ddagger = 53.1 \pm 1.8 \text{ kJ mol}^{-1}$, $\Delta S^\ddagger = 14.6 \pm 7.4 \text{ J mol}^{-1} \text{ K}^{-1}$, and $\Delta G^\ddagger_{298} = 48.7 \pm 0.4 \text{ kJ mol}^{-1}$ (Figure 4b).

After setting up a five-component rotor, our next vision was to generate and operate it in an out-of-equilibrium fashion. On the basis of the rotor components, we combined ligands 2–4 and zinc(II) (Figure 1) with hexacyclen (1), expecting that, in a clean self-sorting reaction, Zn^{2+} would coordinate exclusively to hexacyclen (NetState I). Now the consequential idea was to add an acid (2 equiv) to protonate the complex $[\text{Zn}(\mathbf{1})]^{2+}$, thus liberating Zn^{2+} to join ligands 3 and 4 in a HETTAP⁴³ complex and simultaneously to protonate the amine of ligand 2 to create a pseudorotaxane linkage with ligand 3. Eventually, the combination of both these complexes was expected to furnish NetState-II composed of $[\text{H}(\mathbf{1})]^+$ and rotor $[\text{Zn}(\mathbf{2}\cdot\text{H}^+)(\mathbf{3})(\mathbf{4})]^{2+}$.

As planned, self-sorting of zinc(II) in the presence of 1–4 in a 1:1:1:1 ratio cleanly delivered $[\text{Zn}(\mathbf{1})]^{2+}$ with all other ligands in NetState-I left unassociated, as indicated by ^1H NMR spectroscopy (in dichloromethane- d_2). Upon addition of 2 equiv of TFA, the ^1H NMR spectrum (Supporting Information, Figure S55) showed complete translocation of Zn^{2+} from hexacyclen to ligand 3 and 4 and simultaneous formation of the pseudorotaxane, which eventually generated the rotor (NetState-II). The ESI-MS showed the presence of both complexes $[\text{Zn}(\mathbf{2}\cdot\text{H}^+)(\mathbf{3})(\mathbf{4})]^{2+}$ and $[\text{H}(\mathbf{1})]^+$ by peaks at $m/z = 1908.0$ (doubly charged) and a signal at $m/z = 259.7$ (singly charged) (Supporting Information, Figure S66). Reverse translocation of zinc(II) from rotor 5 back to hexacyclen was readily achieved after addition of 2 equiv of DBU.

When NetState-I was titrated with TFA, from the beginning it showed formation of prerotor $[\text{Zn}(\mathbf{2})(\mathbf{3})(\mathbf{4})]^{2+}$ and only thereafter rotor 5 (Figure 5a). Formation of the assemblies was followed by the distinct ^1H NMR signals of protons 10-H in ligand 4, prerotor, and rotor. Upon addition of 0.3 equiv of acid, 21% of prerotor and 9% of rotor were generated, which furthermore turned into 57% of prerotor and 39% of rotor upon addition of 1.2 equiv of acid and eventually the rotor was fully afforded upon addition of overall 2 equiv of TFA (Figure 5b). This finding suggested that TFA first liberated zinc(II), whereas formation of the pseudorotaxane rotor was rate-limiting.

Eventually, rotor formation was fueled by acid 6, which is expected to initially provide the required protons for the self-assembly of rotor 5. However, after decarboxylation, the strong base $\mathbf{6}^{\text{A}}$ reclaimed the protons, enforcing disassembly of 5 (equation 1).

The fueled process was conveniently traceable by fluorescence spectroscopy (Figure 6a). Upon addition of one equiv of fuel 6 to prerotor $[\text{Zn}(\mathbf{2})(\mathbf{3})(\mathbf{4})]^{2+}$ (showing a weak emission at $\lambda_{\text{em}} = 579 \text{ nm}$), the fluorescence intensity increased continu-

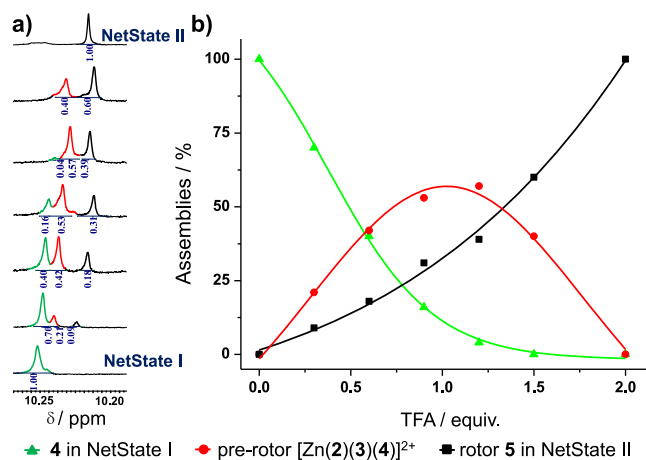


Figure 5. Transformation of NetState-I \rightarrow NetState-II with TFA. (a) The proton 10-H signal (^1H NMR) shows formation of rotor via the intermediate prerotor assembly. (b) The prerotor/rotor is shown at different amounts of TFA.

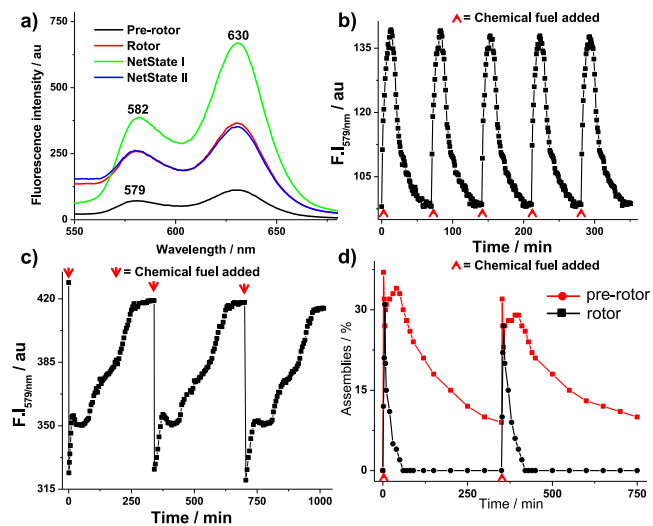
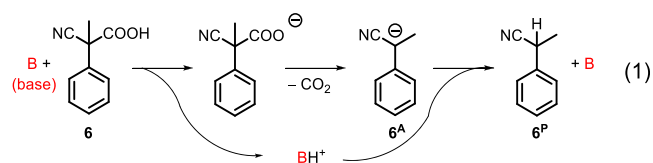


Figure 6. (a) Fluorescence spectra of prerotor, rotor, NetState-I and -II ($c = 1.1 \times 10^{-5} \text{ M}$, CH_2Cl_2 , $\lambda_{\text{exc}} = 350 \text{ nm}$). (b) Off-equilibrium transformation of prerotor $[\text{Zn}(\mathbf{2})(\mathbf{3})(\mathbf{4})]^{2+} \rightarrow$ rotor followed by fluorescence changes at 579 nm vs time upon addition (red arrow) of fuel 6. (c) Out-of-equilibrium transformation of NetState-I \rightarrow NetState-II documented by fluorescence changes at 579 nm vs time upon addition (red arrow) of fuel 6. (d) Two fueled cycles of NetState-I \rightarrow NetState-II \rightarrow NetState-I monitored by ^1H NMR.

ously for the first 14 min, suggesting a slow threading of $\mathbf{2}\cdot\text{H}^+$ into the prerotor (Figure 6b). Over the course of ca. 70 min, the fluorescence intensity then decreased constantly (rotor \rightarrow prerotor), a process that was reproduced over five fuel cycles.

The full transformation NetState-I \rightleftharpoons NetState-II was first followed by fluorescence spectrometry. After 2 equiv of acid 6 had been added to NetState-I ($\lambda_{\text{em}} = 582 \text{ nm}$), the emission intensity decreased drastically within the first minute (Figure 6c) suggesting rapid prerotor formation. Thereafter the

fluorescence intensity increased (1–20 min). In the beginning, the increase may be explained by formation of the more fluorescent rotor from the less fluorescent prerotor, whereas the intermediate drop in the fluorescence intensity (20–75 min) suggests decomposition of the rotor to prerotor. The ensuing slow enhancement of the fluorescence intensity (75–342 min) reflects the decomposition of the prerotor to NetState-I. Three fuel cycles showed the high reproducibility (Figure 6c).

To get direct structural information about the fueled NetState-I \rightleftharpoons NetState-II transformation, the process was followed by ^1H NMR using the signal of proton 10-H. The spectra revealed rapid formation of the rotor with a maximum (31%) reached after 6 min (Figure 6d); then the rotor amount decreased. After 60 min, the rotor had fully decomposed into the prerotor that over 300 min converted to free ligand **4** in NetState-I. Clearly, the reverse Zn^{2+} translocation is much slower than the initial zinc liberation after deprotonation of ligand **2**. Thus, in the forward direction, pseudorotaxane formation was the slow step whereas in the reverse direction the Zn^{2+} transport was slowest.

In conclusion, we demonstrate that the pseudorotaxane motif is orthogonal to the HETTAP and $N_{\text{py}} \rightarrow \text{ZnPor}$ linkages, allowing the integrative use of all these binding motifs to generate a five-component rotor with an exchange frequency of 15.4 kHz (at room temperature). In contrast to fueled homooligomeric assembly,¹⁰ the chemical fueling was instructed for multitasking, instigating two kinetically distinct assembly and disassembly steps in the dissipative rotor formation. Further synchronization of fueled steps constitutes a vital challenge so that complex molecular networks and machinery are efficiently operated in an out-of-equilibrium manner using a single fuel.

■ ASSOCIATED CONTENT

■ Supporting Information

The Supporting Information is available free of charge at <https://pubs.acs.org/doi/10.1021/jacs.1c01948>.

Synthetic procedures and full spectral characterization of all new compounds, binding constants, and kinetic data (PDF)

■ AUTHOR INFORMATION

Corresponding Author

Michael Schmittel – Center of Micro- and Nanochemistry and Engineering, Organische Chemie I, Universität Siegen, D-57068 Siegen, Germany; orcid.org/0000-0001-8622-2883; Email: schmittel@chemie.uni-siegen.de

Authors

Amit Ghosh – Center of Micro- and Nanochemistry and Engineering, Organische Chemie I, Universität Siegen, D-57068 Siegen, Germany

Indrajit Paul – Center of Micro- and Nanochemistry and Engineering, Organische Chemie I, Universität Siegen, D-57068 Siegen, Germany

Complete contact information is available at: <https://pubs.acs.org/doi/10.1021/jacs.1c01948>

Notes

The authors declare no competing financial interest.

■ ACKNOWLEDGMENTS

We are highly indebted to the DFG (Schm 647/20-2) and to Dr. T. Paululat of the University of Siegen. Dedicated to the memory of Professor Siegfried Hünig.

■ REFERENCES

- (1) Kariyawasam, L. S.; Hartley, C. S. Dissipative Assembly of Aqueous Carboxylic Acid Anhydrides Fueled by Carbodiimides. *J. Am. Chem. Soc.* **2017**, *139*, 11949–11955.
- (2) Wood, C. S.; Browne, C.; Wood, D. M.; Nitschke, J. R. Fuel-Controlled Reassembly of Metal-Organic Architectures. *ACS Cent. Sci.* **2015**, *1*, 504–509.
- (3) Fanlo-Virgós, H.; Alba, A.-N. R.; Hamieh, S.; Colomb-Delsuc, M.; Otto, S. Transient Substrate-Induced Catalyst Formation in a Dynamic Molecular Network. *Angew. Chem., Int. Ed.* **2014**, *53*, 11346–11350.
- (4) Biagini, C.; Di Stefano, S. Abiotic Chemical Fuels for the Operation of Molecular Machines. *Angew. Chem., Int. Ed.* **2020**, *59*, 8344–8354.
- (5) Shi, Q.; Chen, C.-F. Step-by-step reaction-powered mechanical motion triggered by a chemical fuel pulse. *Chem. Sci.* **2019**, *10*, 2529–2533.
- (6) Ghosh, A.; Paul, I.; Adlung, M.; Wickleder, C.; Schmittel, M. Oscillating Emission of [2]Rotaxane Driven by Chemical Fuel. *Org. Lett.* **2018**, *20*, 1046–1049.
- (7) Erbas-Cakmak, S.; Fielden, S. D. P.; Karaca, U.; Leigh, D. A.; McTernan, C. T.; Tetlow, D. J.; Wilson, M. R. Rotary and linear molecular motors driven by pulses of a chemical fuel. *Science* **2017**, *358*, 340–343.
- (8) Wilson, M. R.; Solà, J.; Carlone, A.; Goldup, S. M.; Lebrasseur, N.; Leigh, D. A. An autonomous chemically fuelled small-molecule motor. *Nature* **2016**, *534*, 235–240.
- (9) Biagini, C.; Fielden, S. D. P.; Leigh, D. A.; Schaufelberger, F.; Di Stefano, S.; Thomas, D. Dissipative Catalysis with a Molecular Machine. *Angew. Chem., Int. Ed.* **2019**, *58*, 9876–9880.
- (10) Singh, N.; Lainer, B.; Formon, G. J. M.; De Piccoli, S.; Hermans, T. M. Re-programming Hydrogel Properties Using a Fuel-Driven Reaction Cycle. *J. Am. Chem. Soc.* **2020**, *142*, 4083–4087.
- (11) Rieß, B.; Grötsch, R. K.; Boekhoven, J. The Design of Dissipative Molecular Assemblies Driven by Chemical Reaction Cycles. *Chem.* **2020**, *6*, 552–578.
- (12) Tena-Solsona, M.; Rieß, B.; Grötsch, R.; Löhner, F.; Wanzke, C.; Käs Dorf, B.; Bausch, A.; Müller-Buschbaum, P.; Lieleg, O.; Boekhoven, J. Non-equilibrium dissipative supramolecular materials with a tunable lifetime. *Nat. Commun.* **2017**, *8*, 15895.
- (13) Dhiman, S.; Jain, A.; George, S. J. Transient Helicity: Fuel-Driven Temporal Control over Conformational Switching in a Supramolecular Polymer. *Angew. Chem., Int. Ed.* **2017**, *56*, 1329–1333.
- (14) Boekhoven, J.; Hendriksen, W. E.; Koper, G. J. M.; Eelkema, R.; van Esch, J. H. Transient assembly of active materials fueled by a chemical reaction. *Science* **2015**, *349*, 1075–1079.
- (15) Morrow, S. M.; Colomer, I.; Fletcher, S. P. A chemically fuelled self-replicator. *Nat. Commun.* **2019**, *10*, 1011.
- (16) Ragazzon, G.; Prins, L. J. Energy consumption in chemical fuel-driven self-assembly. *Nat. Nanotechnol.* **2018**, *13*, 882–889.
- (17) Mishra, A.; Korlepara, D. B.; Kumar, M.; Jain, A.; Jonnalagadda, N.; Bejagam, K. K.; Balasubramanian, S.; George, S. J. Biomimetic temporal self-assembly via fuel-driven controlled supramolecular polymerization. *Nat. Commun.* **2018**, *9*, 1295.
- (18) Ashkenasy, G.; Hermans, T. M.; Otto, S.; Taylor, A. F. Systems chemistry. *Chem. Soc. Rev.* **2017**, *46*, 2543–2554.
- (19) Maiti, S.; Fortunati, I.; Ferrante, C.; Scrimin, P.; Prins, L. J. Biomimetic temporal self-assembly via fuel-driven controlled supramolecular polymerization. *Nat. Chem.* **2016**, *8*, 725–731.
- (20) Goswami, A.; Saha, S.; Biswas, P. K.; Schmittel, M. (Nano)-mechanical Motion Triggered by Metal Coordination: from Functional Devices to Networked Multicomponent Catalytic Machinery. *Chem. Rev.* **2020**, *120*, 125–199.

- (21) Sluysmans, D.; Stoddart, J. F. Growing community of artificial molecular machinists. *Proc. Natl. Acad. Sci. U. S. A.* **2018**, *115*, 9359–9361.
- (22) Watson, M. A.; Cockroft, S. L. Man-made molecular machines: membrane bound. *Chem. Soc. Rev.* **2016**, *45*, 6118–6129.
- (23) Erbas-Cakmak, S.; Leigh, D. A.; McTernan, C. T.; Nussbaumer, A. L. Artificial Molecular Machines. *Chem. Rev.* **2015**, *115*, 10081–10206.
- (24) McConnell, A. J.; Wood, C. S.; Neelakandan, P. P.; Nitschke, J. R. Stimuli-Responsive Metal-Ligand Assemblies. *Chem. Rev.* **2015**, *115*, 7729–7793.
- (25) Schliwa, M.; Woehlke, G. Molecular motors. *Nature* **2003**, *422*, 759–765.
- (26) Yoshida, M.; Muneyuki, E.; Hisabori, T. ATP Synthase-A Marvellous Rotary Engine of the Cell. *Nat. Rev. Mol. Cell Biol.* **2001**, *2*, 669–677.
- (27) Nakamura, M.; Kishimoto, K.; Kobori, Y.; Abe, T.; Yoza, K.; Kobayashi, K. Self-Assembled Molecular Gear: A 4:1 Complex of Rh(III)Cl Tetraarylporphyrin and Tetra(p-pyridyl)cavitand. *J. Am. Chem. Soc.* **2016**, *138*, 12564–12577.
- (28) Takara, Y.; Kusamoto, T.; Masui, T.; Nishikawa, M.; Kume, S.; Nishihara, H. A single-molecular twin rotor: correlated motion of two pyrimidine rings coordinated to copper. *Chem. Commun.* **2015**, *51*, 2896–2898.
- (29) Scottwell, S. O.; Elliott, A. B. S.; Shaffer, K. J.; Nafady, A.; McAdam, C. J.; Gordon, K. C.; Crowley, J. D. Chemically and electrochemically induced expansion and contraction of a ferrocene rotor. *Chem. Commun.* **2015**, *51*, 8161–8164.
- (30) Nishikawa, M.; Kume, S.; Nishihara, H. Stimuli-responsive pyrimidine ring rotation in copper complexes for switching their physical properties. *Phys. Chem. Chem. Phys.* **2013**, *15*, 10549–10565.
- (31) Shibata, M.; Tanaka, S.; Ikeda, T.; Shinkai, S.; Kaneko, K.; Ogi, S.; Takeuchi, M. Stimuli-responsive Folding and Unfolding of a Polymer Bearing Multiple cerium(IV) Bis(porphyrinate) Joints: Mechano-Imitation of the Action of a Folding Ruler. *Angew. Chem., Int. Ed.* **2013**, *52*, 397–400.
- (32) Ogi, S.; Ikeda, T.; Wakabayashi, R.; Shinkai, S.; Takeuchi, M. A Bevel-Gear-Shaped Rotor Bearing a Double-Decker Porphyrin Complex. *Chem. - Eur. J.* **2010**, *16*, 8285–8290.
- (33) Hiraoka, S.; Hisanaga, Y.; Shiro, M.; Shionoya, M. A Molecular Double Ball Bearing: An Ag(I)-Pt(II) Dodecanuclear Quadruple-Decker Complex With Three Rotors. *Angew. Chem., Int. Ed.* **2010**, *49*, 1669–1673.
- (34) Hiraoka, S.; Okuno, E.; Tanaka, T.; Shiro, M.; Shionoya, M. Ranging Correlated Motion (1.5 nm) of Two Coaxially Arranged Rotors Mediated by Helix Inversion of a Supramolecular Transmitter. *J. Am. Chem. Soc.* **2008**, *130*, 9089–9098.
- (35) Saha, M. L.; Neogi, S.; Schmittel, M. Dynamic heteroleptic metal-phenanthroline complexes: from structure to function. *Dalton Trans.* **2014**, *43*, 3815–3834.
- (36) Biswas, P.; Saha, S.; Paululat, T.; Schmittel, M. Rotating Catalysts Are Superior: Suppressing Product Inhibition by Anchimeric Assistance in Four-Component Catalytic Machinery. *J. Am. Chem. Soc.* **2018**, *140*, 9038–9041.
- (37) Biswas, P.; Saha, S.; Gaikwad, S.; Schmittel, M. Reversible Multicomponent AND Gate Triggered by Stoichiometric Chemical Pulses Commands the Self-Assembly and Actuation of Catalytic Machinery. *J. Am. Chem. Soc.* **2020**, *142*, 7889–7897.
- (38) Goswami, A.; Paululat, T.; Schmittel, M. Switching Dual Catalysis without Molecular Switch: Using A Multicomponent Information System for Reversible Reconfiguration of Catalytic Machinery. *J. Am. Chem. Soc.* **2019**, *141*, 15656–15663.
- (39) Ghosh, A.; Paul, I.; Schmittel, M. Time-Dependent Pulses of Lithium Ions in Cascaded Signaling and Out-of-Equilibrium (Supra)-molecular Logic. *J. Am. Chem. Soc.* **2019**, *141*, 18954–18957.
- (40) Berrocal, J. A.; Biagini, C.; Mandolini, L.; Di Stefano, S. Coupling of the Decarboxylation of 2-Cyano-2-phenylpropanoic Acid to Large-Amplitude Motions: A Convenient Fuel for an Acid-Base-Operated Molecular Switch. *Angew. Chem., Int. Ed.* **2016**, *55*, 6997–7001.
- (41) He, Z.; Jiang, W.; Schalley, C. A. Integrative self-sorting: a versatile strategy for the construction of complex supramolecular architecture. *Chem. Soc. Rev.* **2015**, *44*, 779–789.
- (42) Safont-Sempere, M. M.; Fernández, G.; Würthner, F. Self-Sorting Phenomena in Complex Supramolecular Systems. *Chem. Rev.* **2011**, *111*, 5784–5814.
- (43) Schmittel, M.; Kalsani, V.; Kishore, R. S. K.; Cölfen, H.; Bats, J. W. Dynamic and Fluorescent Nanoscale Phenanthroline/Terpyridine Zinc(II) Ladders. Self-Recognition in Unlike Ligand/Like Metal Coordination Scenarios. *J. Am. Chem. Soc.* **2005**, *127*, 11544–11545.
- (44) Saha, M. L.; De, S.; Pramanik, S.; Schmittel, M. Orthogonality in discrete self-assembly - survey of current concepts. *Chem. Soc. Rev.* **2013**, *42*, 6860–6909.
- (45) Mandal, A. K.; Gangopadhyay, M.; Das, A. Photo-responsive pseudorotaxanes and assemblies. *Chem. Soc. Rev.* **2015**, *44*, 663–676.
- (46) Nicoli, F.; Paltrinieri, E.; Tranfić Bakić, M.; Baroncini, M.; Silvi, S.; Credi, A. Binary logic operations with artificial molecular machines. *Coord. Chem. Rev.* **2021**, *428*, 213589.
- (47) Kwamen, C.; Niemeyer, J. Functional Rotaxanes in Catalysis. *Chem. - Eur. J.* **2021**, *27*, 175–186.
- (48) Xue, M.; Yang, Y.; Chi, X.; Yan, X.; Huang, F. Development of Pseudorotaxanes and Rotaxanes: From Synthesis to Stimuli-Responsive Motions to Applications. *Chem. Rev.* **2015**, *115*, 7398–7501.
- (49) Paul, I.; Goswami, A.; Mittal, N.; Schmittel, M. Catalytic Three-Component Machinery: Control of Catalytic Activity by Machine Speed. *Angew. Chem., Int. Ed.* **2018**, *57*, 354–358.
- (50) Saha, S.; Ghosh, A.; Paululat, T.; Schmittel, M. *Dalton Trans.* **2020**, *49*, 8693–8700.